Escola de Primavera de Transição e Turbulência
Blumenau 2022

ABCM
13th Spring School on Transition and Turbulence
September 19th-23rd, 2022, Blumenau, SC, Brazil

EPTT-2022-0042
Simulation of transitional-turbulent temporal jet via high fidelity CFD

Rodrigo José Albuquerque Barreira (rodrigojabarreira@gmail.com)
Daniel Garcia-Ribeiro
Lucas Dantas Fernandes
Rodrigo Costa Moura
Vinicius Malatesta
Instituto Tecnológico de Aeronáutica - São José dos Campos, SP

Abstract. *The present work aims to report preliminary results of high-fidelity simulations of a transitional-turbulent planar jet. The so-called temporal approach is followed, where triply periodic boundary conditions are used, allowing to capture the evolution of the jet as a whole over time. High fidelity results are obtained by the Large Eddy Simulation (LES) methodology. In particular, we follow the implicit LES approach, where the numerical method's dissipation is relied upon instead of a classical turbulence model. For that, the incompressible Navier-Stokes equations are simulated by the high-order method called Continuous Galerkin (CG) with a suitable dissipative stabilization technique. All simulations were carried out on the open source Nektar++ platform, for Reynolds number 10000, and provided consistent, albeit preliminary, results for the turbulent flow field.*

Keywords: *turbulent jets, implicit LES, spectral element method*

1. INTRODUCTION

The turbulent planar jet is a well-known free shear flow by both numerical and theoretical communities. Free shear flows are known for being utterly susceptible to transition to turbulence due to the Kelvin-Helmholtz instability. Such characteristics prompt the Computational Fluid Dynamics (CFD) community to study the turbulent planar jet to assess fully-developed turbulence, which is a phenomenon whose features are still to be fully comprehended. Turbulent flow regimes are less likely to use simplifying hypotheses and still yield reliable results due to their somewhat chaotic behaviour from a mathematical point of view. So, numerical schemes to solve turbulent flows are computationally expensive. Meteorologists, for example, need to predict the weather faster along with higher accuracy. Thus, high-fidelity numerical schemes are desirable. Smagorinsky (1963) came up with one of the most famous numerical models: the Large Eddy Simulation (LES). This model solves only the largest eddies in a turbulent flow, whilst modelling the smallest ones.

There are two different numerical approaches for a turbulent jet simulation: temporal and spatial. The former simulates how the solution evolves in time (it uses a periodic boundary condition). And the latter simulates how the solution develops in space (it uses in-and-out boundary conditions). The present study uses the temporal approach. Recently, Watanabe *et al.* (2019) performed a Direct Numerical Simulation (DNS) of a temporal planar jet by using the Finite Differences Method (FDM). The initial condition was a LES solution in hopes of a decrease in computational time whilst achieving a result as precise as a complete DNS solution. Moreover, the present study performs a similar simulation but with a different numerical method, aiming to test aspects of numerical stability and the quality of the solution. Thus, Watanabe *et al.* (2019) is deemed the reference work for the results presented here.

The present study uses the Implicit Large Eddy Simulations (ILES) to perform the temporal turbulent planar jet simulation. ILES is also regarded as under-resolved DNS (Moura *et al.* (2015)) since it does not use turbulence models, and the meshes typically used in such cases are not as refined as the ones used in most DNS. This approach is well-suitable for the spectral/hp Element methods due to their properly numerical dissipation, cf. Moura *et al.* (2016, 2017, 2020b, 2022); Mengaldo *et al.* (2018b). By using these methods, Mengaldo *et al.* (2021) performed a simulation of a high-performance road car, Buscariolo *et al.* (2022) performed a simulation of a Formula One front wing, and Wang and Rahmani (2021) performed a simulation of the NASA's Common Research Model (CRM) high-lift configuration near stall. Therefore, the present study uses the Continuous Galerkin (CG) formulation (a spectral/hp formulation) as it is more appropriate for solving the incompressible Navier-Stokes equations. Nevertheless, CG only guarantees C^0 continuity and needs additional numerical dissipation to stabilise the simulation. Thus, this work also tries validating the numerical stabilisation scheme: Gradient Jump Penalty (GJP), first proposed in Burman (2007).

This work is organised as follows. Section 2 shows the methodology used by depicting the mesh generation process as well as the main equations used. Section 3 shows the results and carries out a discussion. Finally, Section 4 concludes the work with some final remarks and future studies.

2. METHODOLOGY

The authors used the open source framework *Nektar++* (Cantwell *et al.* (2015)) in this work to conduct the simulations of incompressible flow in two and three dimensions. The simulations themselves were by adjusting the proper parameters

to be used as inputs to the Nektar++ code. For the validation of the results, the authors aimed at comparing their own results to the ones found in the work of Watanabe *et al.* (2019).

2.1 Initial and boundary conditions

The initial conditions were set in such a way that Equation 1 sets the initial value for the u velocity component, while the initial values for v, w (only for the three-dimensional simulation) and the pressure are null in the beginning. $V_{ref} = 1$ is the reference value for the velocity, $H = 1$ is the initial height of the jet considered and $\theta_j = 0.01H$.

$$\langle u(y) \rangle = \frac{1}{2} V_{ref} + \frac{1}{2} V_{ref} tanh \left(\frac{H - 2|y|}{4\theta_j} \right) \tag{1}$$

As for the boundary conditions, the authors used a triple-periodicity, which means that the value for the velocity components as well as for the pressure in one end of the domain is the same as for the other end in the same direction throughout the simulation. The cross-section of the domain consists of a rectangle of height $10H$ and length $6H$.

2.2 Numerical method

The numerical method chosen for this work is the one called Continous Galerkin (CG), which is a projection included in the family of spectral element methods (SEM). The family of methods consist of approximating the desired solution to a sum of products of expansion functions with coefficients, as it is stated in Eq. (2).

$$u^{\delta}(\mathbf{x}, t) = \sum_{i=0}^{N} \hat{u}_i(t) \Phi(\mathbf{x}) \tag{2}$$

In order to find the values of the coefficients, one must force a condition to the residual that is yielded by substituting the approximated solution into the equation. This condition is achieved by computing the Legendre inner product of the residual with a certain test function and forcing it to be zero, as shown in Eq. (3).

$$\langle v_j(x), R \rangle = 0, \quad j = 1, \ldots, N_{dor} \tag{3}$$

In the case of the CG projection, the test functions must be within the same space as the expansion functions used in the approximation. In formulations like the ones found in the context of SEM, it is possible to change the level of accuracy of the solution by both mesh refinement and polynomial order increasing. During the initial simulations, some refinement tests were conducted leading up to the final mesh and polynomial order adopted in the actual simulations. Here, polynomials of order 2 were used in the approximation throughout the entire domain, which sets the nominal order of accuracy to 3. Subsequent refinements would eventually lead to a DNS, which is not the purpose of this study. The authors want to investigate the behaviour of the CG method for under-resolved turbulent simulation (ILES approach). Also, a polynomial de-aliasing was applied to avoid inexact quadrature errors (Karniadakis and Sherwin (2013)).

2.3 Meshes

The domain was discretized into elements in order to create meshes, which were generated in the software GMSH (Geuzaine and Remacle (2009)). Meshes in both two and three dimensions were made, the latter being created by extruding the aforementioned cross-section by a length of $4H$ along the span-wise direction.

In every case, the half-plane $x - y$ of the domain was broken down into three regions, whose refinements follow different rules. The heights of the elements increase, from the lower boundary of the half-plane, according to geometrical progressions whose ratios are presented in Tab. 1. The heights of the elements used on the boundary of each region are also presented in Tab. 1. The values were chosen in reference to the work of Watanabe *et al.* (2019).

Table 1. Geometrical progression ratios and elements' heights on the boundaries of each domain

Region	Ratio	Initial height of elements
$y = 0$ a $y = \frac{H}{2}$	1.0290	0.013604
$y = \frac{H}{2}$ a $y = \frac{3H}{2}$	1.0010	0.027326
$y = \frac{3H}{2}$ a $y = 5H$	1.3887	0.028295

Figure 1 shows the results of the two-dimensional mesh. The number of elements over the x axis was chosen to be 114. The three-dimensional mesh, on the other hand, was built with 72 elements over the x axis and 48 over the z axis. Furthermore, the fact that the solution is composed of a sum of polynomials makes it possible to increase the number of degrees of freedom (DOF) without refining the mesh any further. For instance, as the polynomial order is 2 for this work, each direction has $2 * n_{el_i}$ DOF, with n_{el_i} being the number of elements along the i_{th} direction.

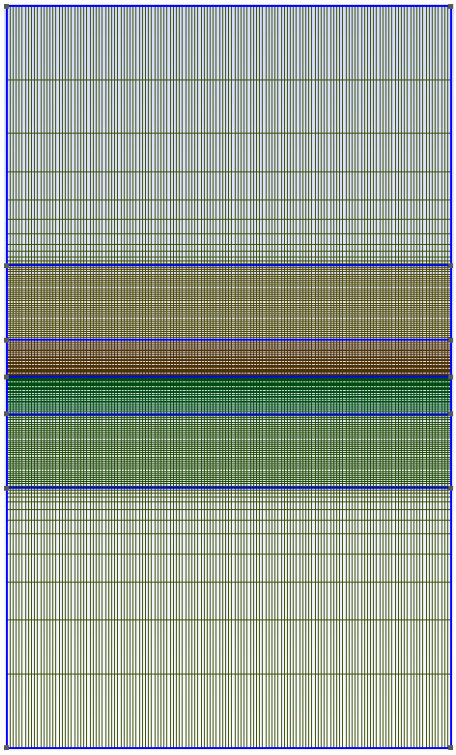

Figure 1. Two dimensional mesh.

2.4 Numerical stabilization scheme

As stated previously, ILES uses meshes that are not as refined as the ones used in DNS, but also, does not seek to employ any turbulence model, which potentially introduces an issue regarding derivatives discontinuity between elements in the context of CG solutions. Therefore, it is necessary to provide the solution with a well-calibrated numerical stabilisation. In the present study, the GJP scheme was employed. The idea behind is to add a dissipative term to the solution to penalise the potential under-resolved scales that may arise due to derivative discontinuity at element boundaries. The penalty parameter τ is then carefully chosen to multiply the dissipative GJP term in order to yield smoother dissipation curves (Moura *et al.* (2022)). Martins *et al.* (2021) conducted a spatial linear diffusion/dissipation analysis to obtain the proper value of τ.

3. RESULTS AND DISCUSSION

Initially, a two-dimensional simulation with initial fluctuations (noise) was conducted in order for the author to understand the code due to its lower computational cost, in a preliminary stage of the setup, to serve as an intermediary step. The author then conducted three-dimensional simulations without any noise. For both simulations, which were carried out with a Reynolds number of 10000, mean velocity profiles for, at least, four different units of time normalised ($\bar{t}$) by the time reference (t_r), defined as the ratio of H and V_{ref}, were plotted and compared to the reference work, as well as the simulation's energy spectra for $\bar{t} = 17$.

3.1 Two-dimensional simulation

Figure 2 shows that, for the two-dimensional simulation, there is a decrease in the mean velocity, which is in line with the fact that the flow is broken down into eddies of decreasing scales. This phenomenon aids in mixing the linear momentum, which in turn, will flatten the mean velocity profile. As may be seen in Fig. 2, the flow transfers energy from the centre line to its boundary regions through a convective diffusion mechanism, i.e. momentum is being transferred from the centerline to the border of the jet. The profile's width for $t = 15t_r$ is greater than the initial profile. Comparing this result with the one in Watanabe *et al.* (2019), there is a difference, which is expected as the absence of the third dimension affects the spreading of the flow.

Figure 3 corroborates the previous statement as it displays a state of the flow at $t = 14t_r$ with the bulk motion moving away from the centre line, decreasing the mean value for the velocity in this region and, consequently, increasing it in the boundary. This is the action of convective diffusion.

Figure 4 presents the two-dimensional energy spectrum at 17 units of the reference time (t_r). This result was computed

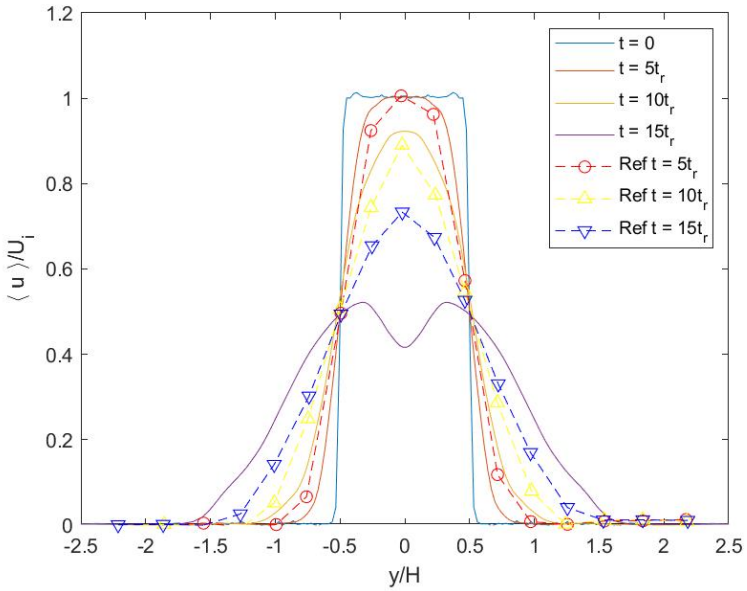

Figure 2. Mean horizontal velocity (u) profile for the two-dimensional simulation and comparison to the three-dimensional simulation of Watanabe *et al.* (2019).

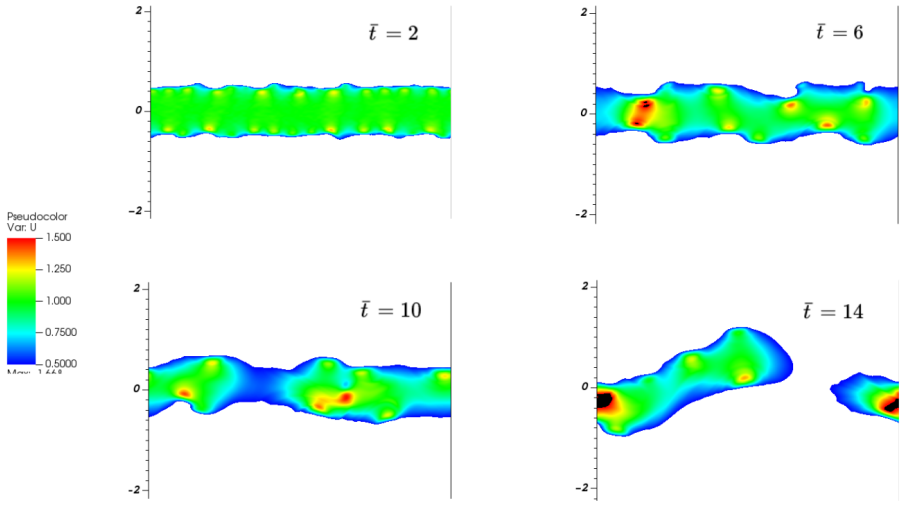

Figure 3. Contours of horizontal velocity (u) according to the color scale as shown on the left-hand side of the plot for four different moments for the two-dimensional simulation.

through the sampling of the u velocity field along the x direction for two y positions, one immediately above the centre line, and the other below, after which the statistical mean was calculated at the instant considered. The results show that increasing eddies, represented by decreasing wavenumbers K_x, present higher energy values, and they decrease as the wavenumber increase. This result is expected, as bigger eddies have more energy, and they tend to share energy to smaller scales, which is in line with the principle of the Energy Cascade Mechanism of Richardson and Lynch (2007).

3.2 Three-dimensional simulation

In the context of three-dimensions, Fig. 5 presents the mean velocity profile for the three-dimensional simulation. The values are closer to the reference values if compared to the two dimensional ones, which was expected, as the addition of the third dimension favours the spreading of the flow. The absence of noise is also thought to have affected the final results negatively, as the transition will take place at a later time than what would be expected if fluctuations were present from the beginning. It is difficult to replicate the exact type of noise employed in Watanabe *et al.* (2019) in the context of SEM since it used a finite differences scheme. Nevertheless, the addition of noise is planned to be carried out in future

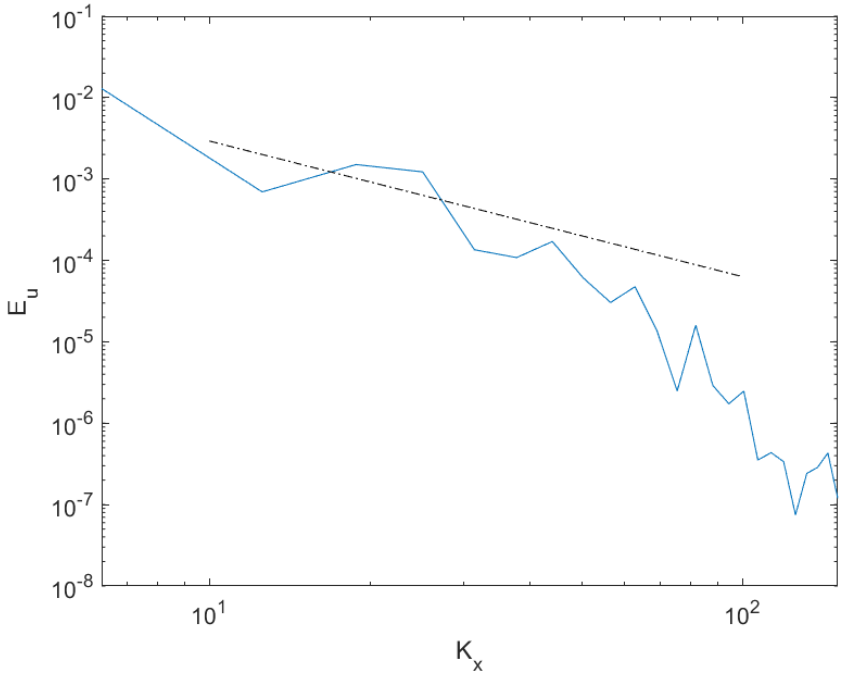

Figure 4. Two-dimensional energy spectrum at instant $\bar{t} = 17$.

works.

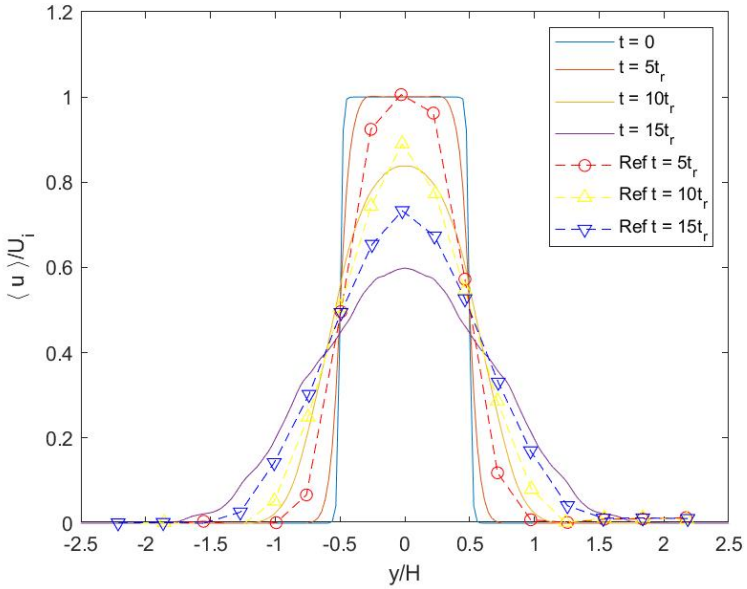

Figure 5. Mean velocity profile for the three-dimensional simulation.

Figure 6 shows iso-surfaces of w velocity in four different times. It may be seen that as time goes by, eddy scales become increasingly smaller, which is in line with the energy cascade mechanism.

The energy spectrum for the three-dimensional simulation at $\bar{t} = 17$ is shown in Fig. 7. This plot is the result of a mean of several one-dimensional energy spectra along the x direction for several z positions, but only for planes on $y = 1$ and $y = -1$. Although the mean u velocity profiles are disparate if compared to the ones found in Watanabe *et al.* (2019), the energy spectrum is consistent with the Kolmogorov's theory, indicating that the simulation is physically consistent with turbulence theory. Therefore, it is possible to emphasise the usefulness of SEM for under-resolved turbulence simulation via Implicit LES.

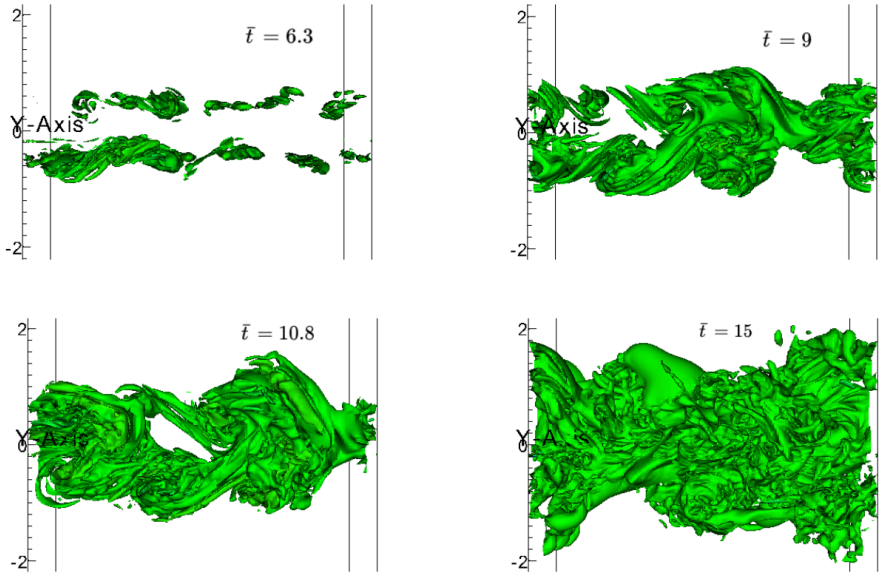

Figure 6. w velocity iso-surfaces for four different moments.

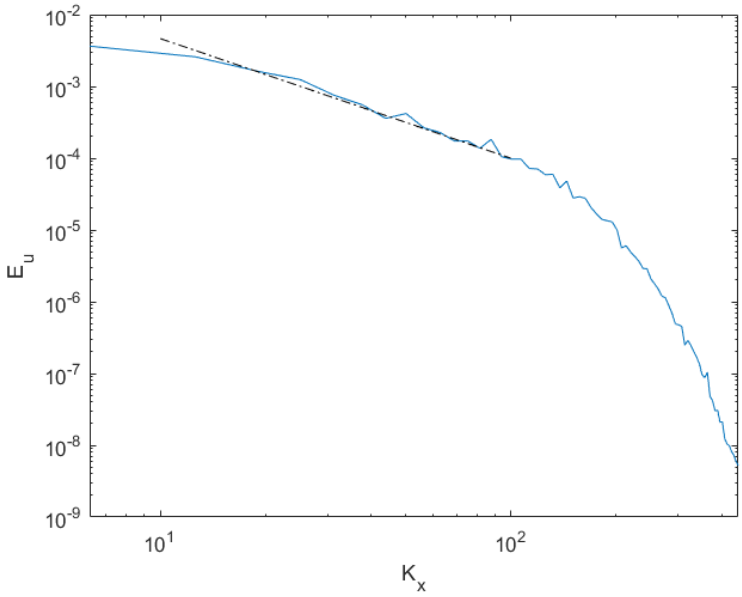

Figure 7. Three dimensional energy spectrum at $\bar{t} = 17$.

4. CONCLUSION

This work aimed at presenting results with hopes of validating the code of the framework used, Nektar++, as well as of studying more thoroughly the numerical method Continous Galerkin as applied to under-resolved turbulence simulation via Implicit LES approaches using adequate numerical stabilization techniques. In this study, the GJP scheme (Moura *et al.* (2015); Mengaldo *et al.* (2018a); Moura *et al.* (2020a)) was chosen and it was observed results consistent with the physics of turbulence. In particular, the three-dimensional energy spectrum followed, for the inertial range, the $\frac{-5}{3}$ slope, as predicted by the Kolmogorov's theory.

The authors expect to run three-dimensional simulations with the presence of noise using the same mesh already exploited in this work, as well as to compare results using meshes with different refinements and approximations with different polynomial orders.

5. ACKNOWLEDGMENTS

The authors gratefully acknowledge funding from São Paulo Research Foundation (FAPESP) under grant 2020/10910-8. In addition, Rodrigo José Albuquerque Barreira acknowledges funding from CNPq (Conselho Nacional de Desenvolvimento Científico e Tecnológico – Brasil) and Daniel Garcia-Ribeiro acknowledges CNPq for the grant 141515/2021-0.

6. REFERENCES

Burman, E., 2007. "Interior penalty variational multiscale method for the incompressible navier–stokes equation: Monitoring artificial dissipation". *Computer methods in applied mechanics and engineering*, Vol. 196, No. 41-44, p. 4045–4058.

Buscariolo, F.F., Hoessler, J., Moxey, D., Jassim, A., Gouder, K., Basley, J., Murai, Y., Assi, G.R. and Sherwin, S.J., 2022. "Spectral/hp element simulation of flow past a formula one front wing: Validation against experiments". *Journal of Wind Engineering and Industrial Aerodynamics*, Vol. 221, p. 104832.

Cantwell, C., Moxey, D., Comerford, A., Bolis, A., Rocco, G., Mengaldo, G., De Grazia, D., Yakovlev, S., Lombard, J.E., Ekelschot, D., Jordi, B., Xu, H., Mohamied, Y., Eskilsson, C., Nelson, B., Vos, P., Biotto, C., Kirby, R. and Sherwin, S., 2015. "Nektar++: An open-source spectral/*hp* element framework". *Computer Physics Communications*, Vol. 192, pp. 205–219.

Geuzaine, C. and Remacle, J.F., 2009. "Gmsh: A 3-d finite element mesh generator with built-in pre-and post-processing facilities". *International journal for numerical methods in engineering*, Vol. 79, pp. 1309–1331.

Karniadakis, G. and Sherwin, S., 2013. *Spectral/hp Element Methods for Computational Fluid Dynamics*. OUP Oxford, 2nd edition. ISBN 9780199671366.

Martins, Y.G.M., Malatesta, V. and Moura, R., 2021. "Numerical study of the flow past an inclined flat plate via spectral/hp element methods with novel stabilization". *Proceedings of the 26th International Congress of Mechanical Engineering*.

Mengaldo, G., De Grazia, D., Moura, R. and Sherwin, S., 2018a. "Spatial eigensolution analysis of energy-stable flux reconstruction schemes and influence of the numerical flux on accuracy and robustness". *Journal of Computational Physics*, Vol. 358, p. 1–20.

Mengaldo, G., Moura, R., Giralda, B., Peiró, J. and Sherwin, S., 2018b. "Spatial eigensolution analysis of discontinuous galerkin schemes with practical insights for under-resolved computations and implicit les". *Computers & Fluids*, Vol. 169, pp. 349–364.

Mengaldo, G., Moxey, D., Turner, M., Moura, R.C., Jassim, A., Taylor, M., Peiro, J. and Sherwin, S., 2021. "Industry-relevant implicit large-eddy simulation of a high-performance road car via spectral/hp element methods". *SIAM Review*, Vol. 63, No. 4, pp. 723–755.

Moura, R., Sherwin, S. and Peiró, J., 2015. "Linear dispersion–diffusion analysis and its application to under-resolved turbulence simulations using discontinuous galerkin spectral/hp methods". *Journal of Computational Physics*, Vol. 298, pp. 695–710.

Moura, R., Silva, A. and Sherwin, S., 2020a. "Eigenanalysis of gradient-jump penalty (gjp) stabilisation for cg". *LASCA research report*. doi:10.13140/RG.2.2.32887.85924.

Moura, R.C., Aman, M., Peiró, J. and Sherwin, S.J., 2020b. "Spatial eigenanalysis of spectral/hp continuous galerkin schemes and their stabilisation via dg-mimicking spectral vanishing viscosity for high reynolds number flows". *Journal of Computational Physics*, Vol. 406, p. 109112.

Moura, R.C., Cassinelli, A., da Silva, A.F., Burman, E. and Sherwin, S.J., 2022. "Gradient jump penalty stabilisation of spectral/hp element discretisation for under-resolved turbulence simulations". *Computer Methods in Applied Mechanics and Engineering*, Vol. 388, p. 114200.

Moura, R.C., Mengaldo, G., Peiró, J. and Sherwin, S.J., 2017. "On the eddy-resolving capability of high-order discontinuous galerkin approaches to implicit les/under-resolved dns of euler turbulence". *Journal of Computational Physics*, Vol. 330, pp. 615–623.

Moura, R.C., Sherwin, S.J. and Peiró, J., 2016. "Eigensolution analysis of spectral/hp continuous galerkin approximations to advection–diffusion problems: Insights into spectral vanishing viscosity". *Journal of Computational Physics*, Vol. 307, pp. 401–422.

Richardson, L.F. and Lynch, P., 2007. *Weather Prediction by Numerical Process*. Cambridge University Press, Cambridge, 2nd edition.

Smagorinsky, J., 1963. "General circulation experiments with the primitive equations". *Monthly Weather Review*, Vol. 91.

Wang, Z. and Rahmani, S., 2021. "Implicit large eddy simulation of the nasa crm high-lift configuration near stall". *Computers & Fluids*, Vol. 220, p. 104887.

Watanabe, T., Zhang, X. and Nagata, K., 2019. "Direct numerical simulation of incompressible turbulent boundary layers and planar jets at high reynolds numbers initialized with implicit large eddy simulation". *Computers and Fluids*, Vol. 194, p. 104314.

7. RESPONSIBILITY NOTICE

The authors are the only responsible for the printed material included in this paper.